

IEICE Proceeding Series

Transitional dynamics in a coupled oscillator system

Kuniyasu Shimizu, Kazuki Ochiai, Tetsuro Endo

Vol. 2 pp. 341-344

Publication Date: 2014/03/18

Online ISSN: 2188-5079

Downloaded from www.proceeding.ieice.org

Transitional dynamics in a coupled oscillator system

Kuniyasu Shimizu[†], Kazuki Ochiai[†], and Tetsuro Endo[‡]

[†]Department of Electrical, Electronics and Computer Engineering, Chiba Institute of Technology
 2-17-1, Tsudanuma, Narashino, Chiba 275-0016, Japan

[‡]Department of Electronics and Bioinformatics, Meiji University
 1-1-1, Higashi-Mita, Tama, Kawasaki, Kanagawa 214-8571, Japan

Email: kuniyasu.shimizu@it-chiba.ac.jp

Abstract—In this study, we conduct a laboratory experiment on a coupled bistable oscillator system for experimental observation of propagating wave phenomena. As a result, we confirm the existence of two different propagating waves in an actual circuit. To compare these propagating waves with our previous work, some numerical results are also given. Moreover, we observe switching solutions that coexist with the propagating waves in the real circuit.

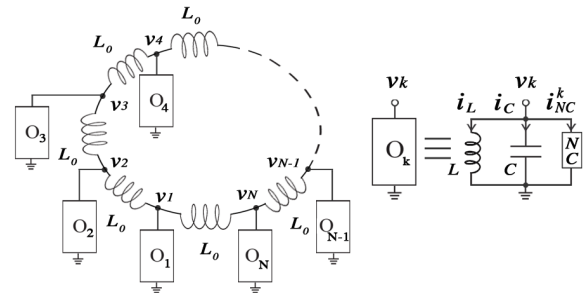


Figure 1: Circuit diagram of coupled bistable oscillators.

1. Introduction

Coupled oscillator systems show rich collective behaviors, and have attracted constant interest for many decades. Intrinsic localized modes (ILMs), also called discrete breathers, are specific excitations that are time-periodic and localized in space. ILMs often appear in various coupled oscillator systems [1, 2]. One widely investigated research area for ILMs are the micromechanical cantilever arrays used for sensing [3, 4]. For such an application, an analysis of the existence and stability of these ILMs, as well as their appropriate control methods, is desirable.

In our previous paper [5], we reported the discovery of two types of propagating wave phenomena existing in a coupled bistable oscillator system. We also provided a formation mechanism for certain propagating wave in the six coupled oscillators. In addition, for the same system, an onset mechanism for the other propagating wave was discussed and a switching phenomenon was investigated [6]. We are now interested in how the excitation related to the ILMs occur in the coupled oscillator system of a real circuit.

In this study, we conduct a laboratory experiment with six coupled bistable oscillators. As a result, we can confirm two different propagating waves can coexist in a real circuit. To compare the propagating waves with our earlier works, some numerical results are presented. Moreover, we observe switching solutions that can coexist with the propagating waves in the real circuit. These attractors can be switched by introducing an external stimulus to the oscillator.

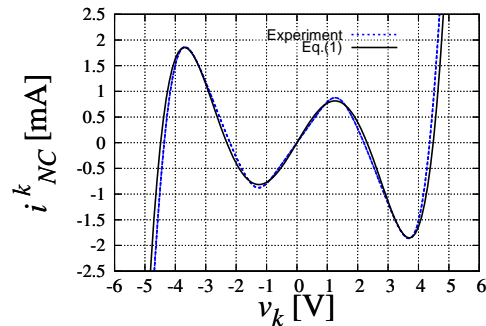


Figure 2: Voltage–current characteristics of the nonlinear conductance NC .

2. Circuit setup

Figure 1 is a schematic circuit diagram for a mutually-coupled bistable oscillator system. The oscillator ($O_k, k = 1, 2, \dots, N$) consists of one inductor (L), one capacitor (C), and one nonlinear conductance (NC). The individual oscillators in the circuit are connected by an inductor (L_0). In this study, we assume voltage–current characteristics of the following fifth-order polynomial form for the NC ,

$$i_{NC}^k = g_1 v_k - g_3 v_k^3 + g_5 v_k^5, \quad g_1, g_3, g_5 > 0. \quad (1)$$

In this case, an isolated oscillator has two steady states [7], making it bistable oscillator. One of the steady states is a limit cycle oscillation, and the other is no oscillation. When we set a large initial value for the oscillator, the limit cycle oscillation is observed. For a small initial value, no oscillation occurs.

From Kirchoff’s law, the circuit equation is written as

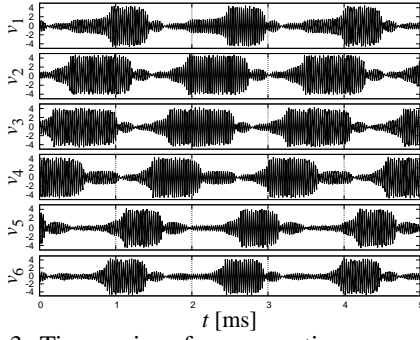


Figure 3: Time series of a propagating wave observed in a real circuit.

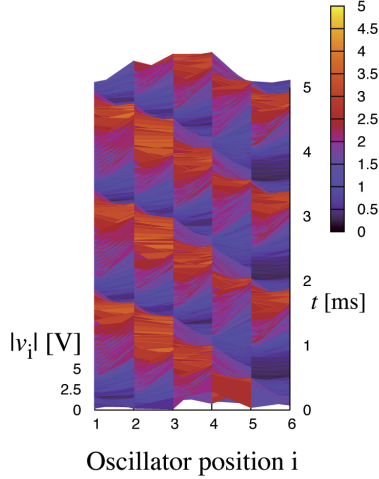


Figure 4: 3D plot of the absolute value of v_i for Fig.3.

follows:

$$\frac{d^2 v_k}{dt^2} + \frac{g_1}{C} \left(1 - \frac{3g_3}{g_1} v_k^2 + \frac{5g_5}{g_1} v_k^4 \right) \frac{dv_k}{dt} + \left(\frac{1}{LC} + \frac{1}{L_0 C} \right) v_k - \frac{1}{L_0 C} (v_{k+1} + v_{k-1}) = 0, \quad (2)$$

$$k = 1, 2, \dots, N \quad (v_0 = v_N, v_{N+1} = v_1).$$

By changing each parameter and variable as:

$$\begin{aligned} t &= t' / \sqrt{(1/LC) + (1/L_0 C)}, \quad v_k = \sqrt[4]{g_1/5g_5} y_k, \\ \varepsilon &\equiv g_1 / \sqrt{(C/L) + (C/L_0)}, \quad \alpha \equiv L/(L + L_0), \\ \beta &\equiv 3g_3 / \sqrt{5g_1 g_5}, \end{aligned} \quad (3)$$

the normalized version of Eq.(2) is represented by the following:

$$\begin{aligned} \dot{\mathbf{x}} &= \mathbf{y} \\ \dot{\mathbf{y}} &= -\varepsilon(\dot{\mathbf{x}} - \frac{1}{3}\beta\dot{\mathbf{x}}_C + \frac{1}{5}\dot{\mathbf{x}}_f) - \mathbf{K}_N \mathbf{x} \end{aligned} \quad (4)$$

$(\cdot = d/dt')$

where $\mathbf{x} = [x_1, x_2, \dots, x_N]^T$, $\mathbf{y} = [y_1, y_2, \dots, y_N]^T$, $\mathbf{x}_C = [x_1^3, x_2^3, \dots, x_N^3]^T$, $\mathbf{x}_f = [x_1^5, x_2^5, \dots, x_N^5]^T$, and

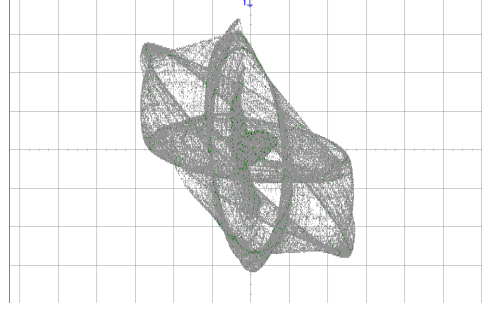


Figure 5: The Lissajous orbit on the $v_2 - v_1$ plane of the propagating wave in Fig.3. The horizontal axis is v_2 [1.4V/div], and the vertical axis is v_1 [1.4V/div].

$$\mathbf{K}_N = \begin{bmatrix} 1 + \alpha & -\alpha & & & -\alpha \\ -\alpha & 1 + \alpha & -\alpha & & \\ & & \ddots & \ddots & \ddots & \mathbf{0} \\ \mathbf{0} & & & \ddots & \ddots & -\alpha \\ -\alpha & & & & -\alpha & 1 + \alpha \end{bmatrix}.$$

The parameter ε (> 0) corresponds to the degree of nonlinearity. The parameter α ($0 \leq \alpha \leq 1$) is a coupling factor. The parameter β controls the amplitude of oscillation.

For the realization of the circuit shown in Fig.1, we design an *NC* consisting of an OP-amp, resistors, and diodes using SPICE. The experimentally-measured curve for the *NC*, and the characteristic curve obtained from Eq.(1) for $g_1 = 1.000 \times 10^{-3}$, $g_3 = 2.216 \times 10^{-4}$, and $g_5 = 8.645 \times 10^{-6}$, are shown by the dotted and solid curves in Fig.2, respectively. From the figure, it can be seen that this study is intended to investigate the case of $\beta = 3.20$, which was usually assumed for the numerical results [5,6].

For this study, we set the circuit elements as $C = 14$ [nF], $L = 2$ [mH], and $L_0 = 13.33$ [mH] (the corresponding parameters are $\varepsilon = 0.36$ and $\alpha = 0.13$). Therefore, the oscillatory frequency of the limit cycle for the isolated oscillator becomes nearly the resonant frequency ($f_0 = 30$ [kHz]).

3. Transitional dynamics

In this section, we give experimental observations for the transitional dynamics of the six coupled oscillator system. First, we investigate the two kinds of propagating wave phenomena, which relate to traveling ILMs. Then, a switching solution which seems to be a kind of stationary ILM, is presented.

3.1. Propagating waves

Figure 3 presents the time series for a propagating wave. To demonstrate the spatiotemporal pattern, we show a 3D plot of absolute values of v_i , $i = 1, 2, \dots, 6$ in Fig.4, where the brighter colors indicates a larger amplitude of oscillation. It is clear that the propagating wave is created by

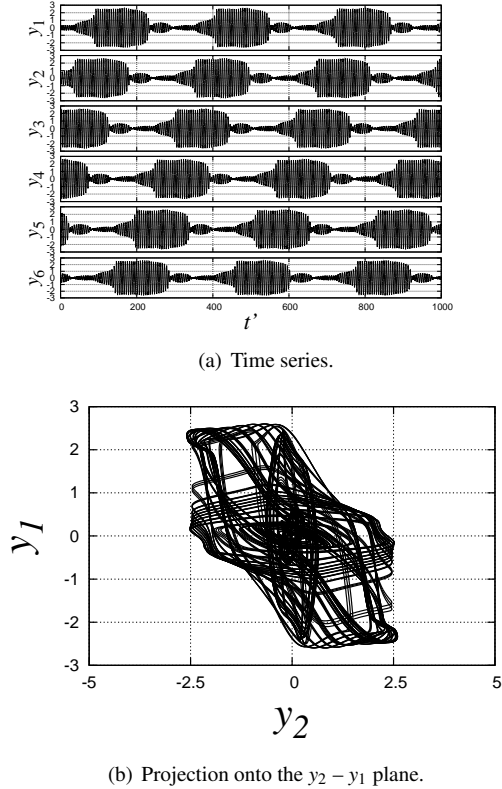


Figure 6: Numerical results for a propagating wave ($\alpha = 0.13, \beta = 3.2$, and $\varepsilon = 0.36$).

several adjacent oscillators oscillating with a large amplitude, and that part of the large amplitude oscillation propagates in one direction with a constant speed. In addition, we plot Lissajous orbit on the $v_2 - v_1$ plane for the propagating wave in Fig.5. It can also be shown that the solution can propagate in the opposite direction with a reversely symmetrical initial state.

To compare the propagating wave with our earlier works, we show the numerical results of Eq.(4) for $\alpha = 0.13, \beta = 3.2$, and $\varepsilon = 0.36$. When the initial condition is set so as to achieve a periodic oscillation called a type 2 standing wave [6], the propagating wave (PW) appears in the homogeneously coupled array. Figures 6 (a) and (b) present the time series and the Lissajous projection onto the $y_2 - y_1$ plane of the solution, respectively. Note that $y_i, i = 1, 2, \dots, 6$ is the normalized state variable of the voltage v_i as defined in Eq.(3). Comparing with the experimental results, it can be seen that the graphs resemble each other. Therefore, the experimentally obtained propagating wave corresponds to the numerically obtained propagating solution.

Next, we investigate other propagating wave phenomena of the circuit. With the same parameter set for PW, we can observe another propagating wave as depicted in Fig.7. It should be noted that this other propagating wave coexists with PW. From the Figs.7 (a) and (b), it can be seen that part of the large amplitude oscillation also propagates in

one direction with a constant speed. However, the waveform and the Lissajous orbit differ considerably from PW. In particular, the sojourn time for the larger amplitude of oscillation is longer than that of PW. For this reason, the propagating wave in Fig.7 is distinguishable from PW.

3.2. Switching phenomena

Figure 8 shows some transitional dynamics which coexist in the real circuit with the two propagating waves previously described. From the figure, it would appear that the oscillatory waveforms change almost periodically between three pairs of the voltage, namely $v_1 - v_4, v_2 - v_6$, and $v_3 - v_2$. This means that one oscillator of each pair oscillates with larger amplitude of oscillation, while the other oscillates with the smaller amplitude oscillation. This phenomenon continues almost periodically and successively, and for this reason we call such a solution “switching solution”. Although we present only one switching solution here due to space limitations, we confirm that five different switching solutions coexist with the propagating waves.

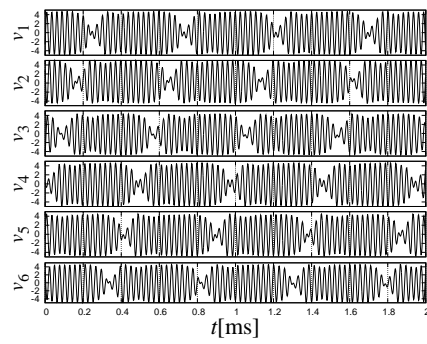
4. Conclusions

In this study, we reported experimental observations for propagating wave phenomena in six coupled bistable oscillators. Compared with the numerical results, one of the observed propagating waves corresponds to the numerically obtained solution which originates from a type 2 standing wave [6]. However, in addition, we confirm the discovery of another propagating wave which coexists with the original propagating wave. The experimental results demonstrate the robustness of such propagating wave phenomena, because characteristic variations and thermal noise are inevitable in a real circuit. Moreover, we also observed switching solutions which coexist with the propagating waves in the real circuit. These transitional dynamics can be controlled by introducing an external DC stimulus to the oscillator.

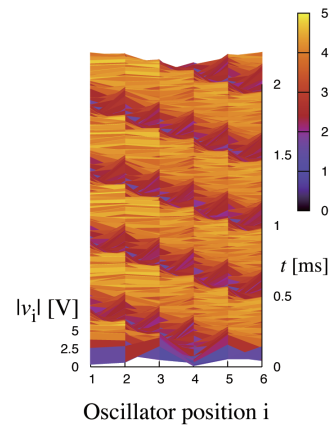
References

- [1] M. Sato, B. E. Hubbard, and A. J. Sievers, “Colloquium: Nonlinear energy localization and its manipulation in micro mechanical oscillator arrays,” *Reviews of Modern Physics*, Vol.78, 2006.
- [2] S. Flach, and A. V. Gorbach, “Discrete breathers – Advances in theory and applications,” *Physics Reports*, Vol.467, pp.1–116, 2008.
- [3] M. Kimura, and T. Hikiyara, “Capture and release of traveling intrinsic localized mode in coupled cantilever array,” *Chaos*, 19, 013138, 2009.
- [4] D. Brake, and V. Putkaradze, “Simplified models for Intrinsic localized mode dynamics,” *Proc. of 2012 NOLTA*, pp.411–414, 2012.

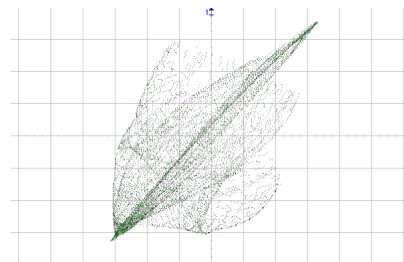
- [5] K. Shimizu, M. Komuro, and T. Endo, “Onset of the propagating pulse wave in a ring of coupled bistable oscillators,” *Nonlinear Theory and Its Applications*, IEICE, vol.2, no.1, pp.139–151, 2011.
- [6] K. Kamiyama, M. Komuro, and T. Endo, “Bifurcation analysis of the propagating wave and the switching solutions in a ring of six-coupled bistable oscillators – bifurcation starting from type2 standing wave solution,” *Inter. Jour. of Bifurcation of Chaos*, vol.22, no.5, 1250123, 2012.
- [7] T. Endo, and T. Ohta, “Multimode oscillations in a coupled oscillator system with fifth-power nonlinear characteristics,” *IEEE Trans. on Circuit and Systems*, vol.CAS-27, no.4, 1980.



(a)



(b)



(c)

Figure 7: Other propagating wave phenomenon in the real circuit. (a) Time series. (b) 3D plot of the $|v_i|$. (c) Lissajous orbit on the $v_2 - v_1$ plane. The horizontal axis is v_2 [1.4V/div], and the vertical axis is v_1 [1.4V/div].

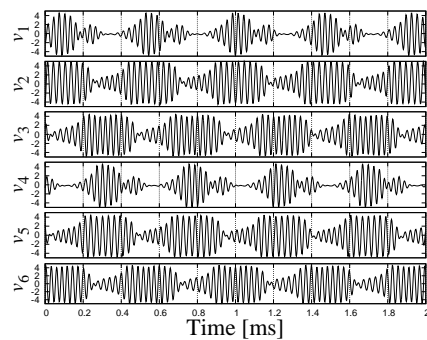


Figure 8: Time series of a switching solution in the real circuit.